2006

Effects of Dissolved Air on Subcooled Flow Boiling of a Dielectric Coolant in a Microchannel Heat Sink

T. Chen

S V. Garimella
Purdue University, sureshg@purdue.edu

Chen, T. and Garimella, S V., "Effects of Dissolved Air on Subcooled Flow Boiling of a Dielectric Coolant in a Microchannel Heat Sink" (2006). *CTRC Research Publications.* Paper 285.
http://dx.doi.org/10.1115/1.2351905

Effects of Dissolved Air on Subcooled Flow Boiling of a Dielectric Coolant in a Microchannel Heat Sink

Tailian Chen

Suresh V. Garimella[1]
e-mail: sureshg@purdue.edu

Cooling Technologies Research Center,
School of Mechanical Engineering,
Purdue University,
West Lafayette, IN 47907-2088

The effects of dissolved air in the dielectric liquid FC-77 on flow boiling in a microchannel heat sink containing ten parallel channels, each 500 μm *wide and* 2.5 mm *deep, were experimentally investigated. Experiments were conducted before and after degassing, at three flow rates in the range of* 30–50 ml/min. *The dissolved air resulted in a significant reduction in wall temperature at which bubbles were first observed in the microchannels. Analysis of the results suggests that the bubbles observed initially in the undegassed liquid were most likely air bubbles. Once the boiling process is initiated, the wall temperature continues to increase for the undegassed liquid, whereas it remains relatively unchanged in the case of the degassed liquid. Prior to the inception of boiling in the degassed liquid, the heat transfer coefficients with the undegassed liquid were* 300–500 *% higher than for degassed liquid, depending on the flow rate. The heat transfer coefficients for both cases reach similar values at high heat fluxes* ($>$120 kW/m^2) *once the boiling process with the degassed liquid was well established. The boiling process induced a significant increase in pressure drop relative to single-phase flow; the pressure drop for undegassed liquid was measured to be higher than for degassed liquid once the boiling process became well established in both cases. Flow instabilities were induced by the boiling process, and the magnitude of the instability was quantified using the standard deviation of the measured pressure drop at a given heat flux. It was found that the magnitude of flow instability increased with increasing heat flux in both the undegassed and degassed liquids, with greater flow instability noted in the undegassed liquid.* [DOI: 10.1115/1.2351905]

Introduction

Flow boiling in microchannels provides very high rates of heat transfer in a compact cooling volume, offering an attractive cooling option for modern electronics. Because of their superior electrical and chemical properties, Fluorocarbon fluids, such as FC-77 from 3M Fluorinerts [1], are the leading candidates for such applications. Previous studies have shown that the presence of noncondensible gases, such as air, in the liquid can affect the boiling process. In early work by Torikai et al. [2], dissolved air was found to reduce bubble nucleation temperature in water. In a study of the bubble incipience phenomenon and hysteresis in flow boiling of Freon-113, Murphy and Bergles [3] also found a reduced wall temperature requirement for bubble incipience. You et al. [4] observed that the effect of dissolved air on the heat transfer rate from a 0.51 mm dia cylinder in a pool of FC-72 was evident only at high air content (0.0056 mole/mole); the critical heat flux (CHF) was measured to be 2.5 times higher due to the dissolved air. No effect of dissolved air was discerned at air content of $<$0.0025 mole/mole. Hong et al. [5] found that the heat transfer enhancement due to dissolved air decreases with increasing heat flux and attributed this decrease to air depletion in the liquid near the wall at high wall temperatures. The effects of dissolved gas in flow boiling heat transfer of water and heptane in an annular stainless steel tube of 10.7 mm dia were investigated by Muller-Steinhagen et al. [6]. They reported that heat transfer was enhanced and the temperature for bubble incipience was reduced as a result of the presence of dissolved gas, with the enhancement in heat transfer being much less pronounced for water.

Few studies have considered the effect of dissolved gas on flow boiling in microchannels. Steinke and Kandlikar [7] noted that dissolved air in water led to a slight reduction in the heat transfer rate, possibly due to an insulating gas layer being formed at the wall. There would appear to be an apparent inconsistency in the dissolved gas effect at reduced channel sizes, compared to observations in previous studies in conventional geometries. There is a clear need for further study of the effects of dissolved gas in flow boiling in microchannels, particularly for dielectric fluids such as Fluorinert fluids (from 3M), which are characterized by very high levels of air solubility. Dielectric fluids are preferred to water in applications where electronics are exposed to the coolant fluid.

An experimental investigation of the effects of dissolved air on flow boiling heat transfer of the Fluorinert liquid FC-77 (with a Prandtl number of 16.4 at the inlet temperature of 40°C) in a microchannel heat sink is reported in the present work to address this need.

Experimental Facility

Test Loop. The experimental test loop is shown in Fig. 1. A magnetically coupled gear pump GA-180 drives the coolant through the loop. Tests were conducted at three flow rates each for the undegassed and degassed liquid, 30, 40, and 50 ml/min, corresponding to mass fluxes of 70, 93, and 116 kg/m^2 s. The Reynolds number at the channel inlet is 61, 81, and 101, respectively, for the three flow rates. A precision low-flow-rate flow meter (Model S-114, McMillan Company) was used to monitor the flow rate. A preheater installed upstream of the test section controls the

[1]Author to whom correspondence should be addressed.

Contributed by the Electronic and Photonic Packaging Division of ASME for publication in the JOURNAL OF ELECTRONIC PACKAGING. Manuscript received July 11, 2005; final manuscript received February 1, 2006. Review conducted by Guo-Quan Lu.

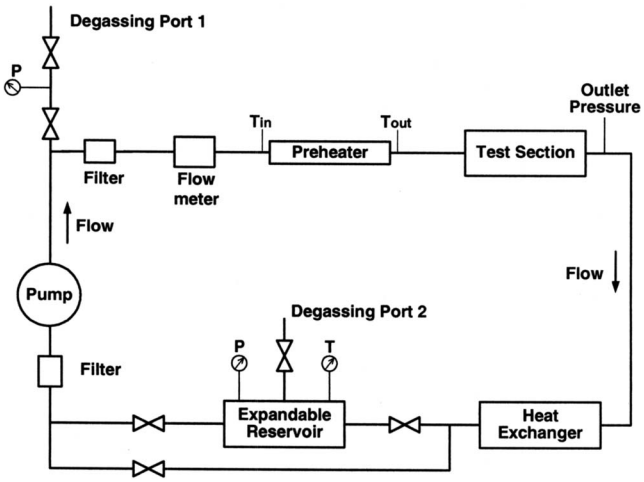

Fig. 1 Experimental system

degree of subcooling in the liquid at the entrance to the microchannels. The inlet temperature for all cases reported in this work was maintained at 40°C.

Under ambient conditions, FC-77 contains 41% of air by volume; this implies that a unit volume of FC-77 liquid contains 0.41 unit volume of air at standard pressure and temperature, which is equivalent to an air concentration of 283 parts per million (ppm). For reference, the air content in water under similar conditions is only 8.25 ppm. In order to fully degas the liquid while maintaining the desired system operating conditions (pressure and temperature), a custom-built degassing scheme is devised and implemented in this work. As shown in Fig. 2, an expandable container was used as a reservoir to facilitate the degassing of the coolant. The constraint mechanism shown in Fig. 2 constrains the expansion and contraction of the reservoir. The reservoir was tested to be leak-free and then filled with liquid FC-77. Degassing was performed by repeatedly evacuating the reservoir of air (and FC-77 vapor) from the top using a vacuum pump; a period of 5–10 min was allowed between evacuations for air diffusion from the liquid into the open volume in the reservoir. The temperature and pressure change in the reservoir are monitored during the evacuation process, and the fluid is considered fully degassed only when the pressure in the reservoir remains at its maximum vacuum level and is unchanged with time. This maximum vacuum

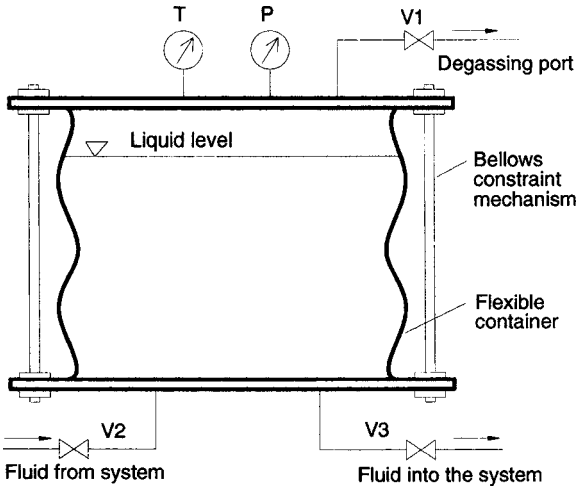

Fig. 2 Schematic of the expandable reservoir used to degas the fluid

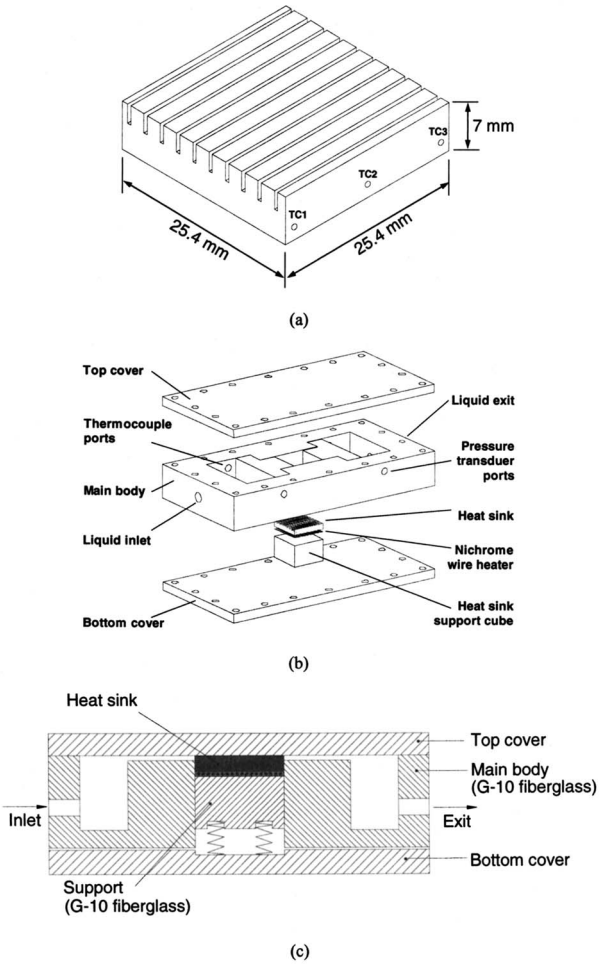

Fig. 3 Details of (*a*) the microchannel heat sink, (*b*) the heat sink test section used in the experiments, and (*c*) cross section of the test section assembly in the flow direction

level of the reservoir was recorded to be 95.5 kPa (28.2 in. of Hg) at a room temperature of 23°C, which is equivalent to a reservoir pressure of 5760 Pa. This is very close to the vapor pressure of FC-77 of 5600 Pa at room temperature. The oxygen content of degassed liquid was measured using an oxygen detector (Model 407510 by Extech Instruments) to be <3 ppm, which is equivalent to 0.000215 mole/mole of air content (0.022% by volume). Therefore, it is considered a satisfactory level of degassing.

An additional degassing port is also provided in the test loop as shown in Fig. 1. This port is used to evacuate air from the test loop prior to charging it with liquid. When the liquid in the test loop and reservoir is degassed, the constraint mechanism on the reservoir is adjusted to allow the bellows to contract such that the pressure in the test section is maintained at atmospheric pressure.

Test Section. The test piece is a microchannel heat sink machined from oxygen-free copper. As shown in Fig. 3(*a*) the heat sink has dimensions of 25.4 mm×25.4 mm×7 mm. The heat sink contains ten microchannels, each of width 504 μm, and depth 2.5 mm, extending the length of the heat sink. Thermocouples are inserted at three locations in the lengthwise direction underneath the microchannels along the center of the test section, as shown in Fig. 3(*a*). The thermocouples are located at a distance of 3.1 mm below the bottom of microchannels, with TC_1 being 2 mm from the inlet in the flow direction, TC_2 in the middle, and TC_3 being 2 mm before the exit. A 25 mm square resistance heater constructed with a serpentine nichrome wire is attached to

the bottom of the copper heat sink to provide heat input to the microchannels. The resistance of the nichrome wire heater is measured to be 16.5 Ω at room temperature. In view of the small temperature dependence of resistance for nichrome (0.0004 Ω/Ω K), the resistance change for the temperature range encountered in this work was only 0.04 Ω/Ω so that an assumption of temperature-independent resistance was justified.

The copper heat sink is housed in the test section shown in Fig. 3(*b*). The test section consists of a main body, top and bottom covers, and a heat sink support cube. The main body and support cube are made of G-10 fiberglass, whereas the top and bottom covers are made of transparent plastic. These materials have very low thermal conductivities and provide adequate insulation. The main body contains inlet and outlet plenums to distribute the flow into the microchannels. Two pressure taps and two thermocouples located in the plenums measure the pressure drop and temperature rise across the microchannel test section, respectively. Pressure drop was measured using a differential pressure transducer (OMEGA PX2300-0.5BDI), which was zero adjusted prior to use. The heat sink support cube is supported by four springs to eliminate any gaps between the heat sink and the top cover. A groove on one side of the support cube allows access for the electrical leads of the nichrome heater and thermocouple wires.

Data Analysis

The measured temperatures at the three locations (TC_1, TC_2, TC_3) underneath the microchannels shown in Fig. 3(*a*) were first corrected to obtain the three corresponding wall temperatures as

$$T_{w,i} = T_{\mathrm{TC},i} - \frac{\dot{q}d}{Ak_{cu}}, \quad i = 1,2,3 \tag{1}$$

The average wall temperature was calculated by averaging these three wall temperatures. Since the wall temperatures at the three locations differ very little (by $<1.5\,^{\circ}\mathrm{C}$) except at very high heat fluxes, the log mean temperature difference (LMTD) represents the wall-to-fluid temperature difference:

$$\Delta T_{\mathrm{LMTD}} = \frac{T_{\mathrm{out}} - T_{\mathrm{in}}}{\ln\left(\dfrac{T_w - T_{\mathrm{in}}}{T_w - T_{\mathrm{out}}}\right)} \tag{2}$$

During single-phase flow prior to the inception of boiling in the microchannels, the sensible heat gain by the liquid is given by

$$\dot{q}_{sp} = \rho Q C_P (T_{\mathrm{out}} - T_{\mathrm{in}}) \tag{3}$$

and the difference between the measured input power and the sensible heat gain by the liquid is denoted as the heat loss due to conduction losses through the housing and insulation

$$\dot{q}_{\mathrm{Loss}}(T_w) = \dot{q}_{\mathrm{input}} - \dot{q}_{sp} \tag{4}$$

The heat loss determined by Eq. (4) was found to increase linearly with wall temperature, according to

$$\dot{q}_{\mathrm{Loss}}(T_w) = 0.1519T_w - 5.7121 \tag{5}$$

As would be expected, the variation of wall temperature with input heat flux decreased greatly once boiling was initiated. However, the heat losses in the two-phase regime are still dominated by conduction through the housing and insulation, and can be calculated using Eq. (5). The energy gained by the liquid during the boiling process can thus be determined as

$$\dot{q}_{tp} = \dot{q}_{\mathrm{input}} - \dot{q}_{\mathrm{Loss}}(T_w) \tag{6}$$

The heat transfer coefficients for single- and two-phase flow are thus readily calculated using Eqs. (7) and (8), respectively,

$$h_{sp} = \frac{\dot{q}_{sp}}{A \cdot \Delta T_{\mathrm{LMTD}}} \tag{7}$$

Table 1 Boiling incipience temperature (FC-77, T_{sat}=97 °C at 1 atm)

Flow rate (m1/min)		30	40	50
Boiling incipience temperature (°C)	Degassed	100.1	103.5	105.5
	Undegassed	73.0	75.3	78.5

$$h_{tp} = \frac{\dot{q}_{tp}}{A \cdot (T_w - T_{\mathrm{sat}})} \tag{8}$$

Uncertainty Analysis

Uncertainties in the measured quantities presented in this work include ±1% in flow rate, ±0.5 °C in wall temperature, and 0.25% (8.6 Pa) in the pressure drop measurement, compared to measured values in the range of 170–290 Pa in the two-phase regime. The uncertainty in temperature and flow rate measurement leads to an uncertainty in the single-phase heat transfer rate computed using Eq. (3) of 4.9–38.9 % following the approach of Kline and McClintock [8]; the larger percent uncertainties occurred at the lower wall temperatures primarily due to lower heat transfer rates at lower wall temperatures. For two-phase flow, the heat transfer rate obtained by Eq. (6) has two sources of uncertainty: input power, $\dot{q}_{\mathrm{in}}$ and heat loss, $\dot{q}_{\mathrm{Loss}}$. Combination of these two sources gives rise to total uncertainties in the range of 5.0–7.1 %.

Results and Discussion

Bubble Incipience. The wall temperatures at which boiling incipience is observed are summarized in Table 1 for the undegassed and degassed cases. For the fully degassed liquid, some degree of superheat is required for bubble incipience, with the amount of superheat increasing with increasing flow rate. For the undegassed liquid, on the other hand, bubbles are observed in the microchannels well before the saturation temperature is reached. An increased flow rate suppresses bubble incipience in the undegassed liquid as well. Chen [9] attributed this dependence on flow rate to a thinning of the thermal boundary layer at the wall as the flow rate is increased.

It is instructive to examine the modified Young-Laplace equation for a bubble embryo in equilibrium to further understand the lowered temperature for bubble incipience due to dissolved air in the liquid

$$P_v + P_g = P_l + \frac{2\sigma}{r} \tag{9}$$

in which the left-hand side is the total pressure inside the bubble and P_g is the component of pressure due to dissolved air in the liquid (zero for degassed liquid). The right-hand side represents the total resistance to bubble growth due to the bulk liquid pressure and the surface tension. It is noted that vapor pressure P_v and surface tension σ are temperature dependent, according to 3M Fluorinerts [1],

$$P_v(T) = 0.0011T^4 - 0.0667T^3 + 7.5549T^2 - 2.3808T + 2266.5 \tag{10}$$

$$\sigma(T) = \frac{17.9 - 0.122T}{1000} \tag{11}$$

The bulk liquid can be assumed to be at atmospheric pressure. In order for a bubble to grow from its embryonic size, the left-hand side of Eq. (9) must exceed the right-hand side. In order to determine the temperature at which this condition is satisfied, the initial bubble embryo radius r must be known. Hsu [10] suggested that the initial bubble size is on the order of 1–100 μm. With a known embryo radius r, the value $(P_l + 2\sigma/r)$ at different tempera-

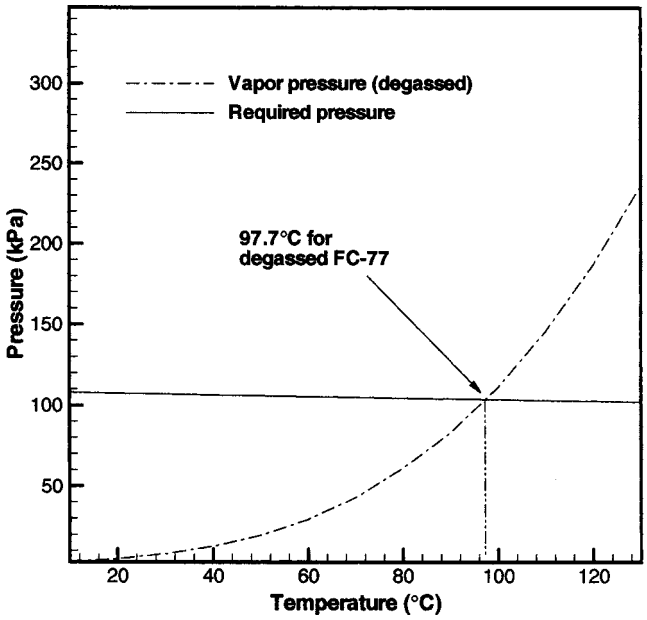

Fig. 4 Prediction of bubble incipience temperature for degassed and undegassed FC-77 (bulk liquid pressure is 1 atm, and the bubble embryo radius is 5.0 μm)

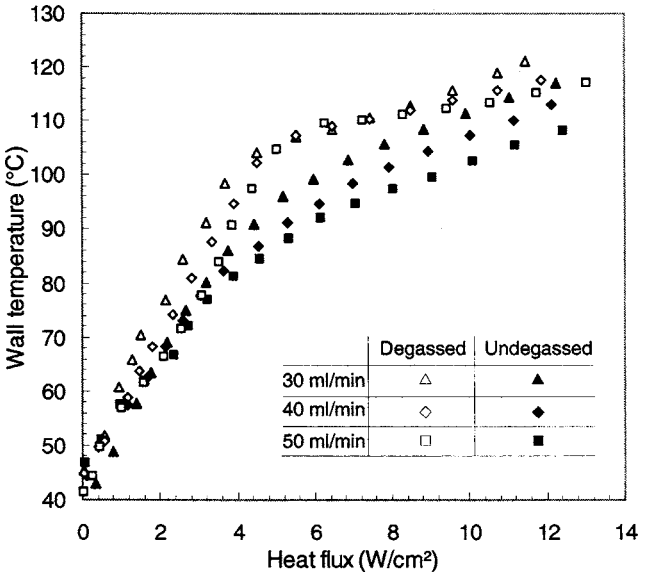

Fig. 5 Wall temperature measured at different heat fluxes for both degassed and undegassed cases

tures can be evaluated and is plotted in Fig. 4 (solid line) with $r = 5$ μm. For the degassed liquid, P_g is zero, and the vapor pressure P_v is the only force available to overcome the resistance to bubble initiation. The vapor pressure of FC-77 given in Eq. (10) is plotted in Fig. 4 (dashed dotted line). The intersection between the two lines represents the temperature required (97.7°C) for a bubble to grow from its embryo in the degassed liquid. For a bubble embryo size range of 1–100 μm, this temperature was found to range from 96 to 100°C. The modified Young-Laplace equation is thus seen to predict a required temperature for bubble nucleation in the degassed liquid that is in close agreement with the boiling point of 97°C for FC-77 [1].

For the undegassed liquid, on the other hand, the pressure P_g in Eq. (9) is not zero. In order to determine this additional pressure, the air concentration c_g in the undegassed liquid must be known. It is noted that one mole of liquid has a volume

$$\mathcal{V}_{\text{mole},l} = \frac{M_l}{\rho_l} \tag{12}$$

As the undegassed liquid is in equilibrium with ambient air, the dissolved air in one mole of liquid has a volume at standard conditions of

$$\mathcal{V}_{\text{mole},g} = \frac{(P_{\text{atm}} - P_{v0})H_0 M_g}{\rho_g} \tag{13}$$

in which H_0 is Henry's constant. It is known from 3M Fluorinerts [1] that air solubility of FC-77 is 41% by volume under standard conditions; that is,

$$\mathcal{V}_{\text{mole},g}/\mathcal{V}_{\text{mole},l} = 0.41 \tag{14}$$

Solving Eqs. (12)–(14) for Henry's constant, the air concentration can be calculated using

$$c_g = (P_{\text{atm}} - P_{v0})H_0 \tag{15}$$

and is determined to be 0.00405 mole/mole.

The concentration of air inside a bubble embryo may be estimated as it grows in the undegassed liquid. The experimental results in Table 1 show a bubble incipience temperature of 73–78°C for the three flow rates considered. At these temperatures, the required pressure for bubble incipience (to overcome the bulk liquid pressure and surface tension) represented by the solid line in Fig. 4 is ≈105 kPa. The vapor pressure of FC-77 at this temperature is ≈50 kPa (Fig. 4). The partial pressure of air inside the bubble must at least equal the difference between the required pressure for bubble incipience and the partial pressure of vapor inside a bubble, i.e., 55 kPa. This indicates that the molar concentration of air inside the bubble is greater than that of the vapor. This analysis is further supported by the heat transfer behavior discussed in the next section.

Heat Transfer. The wall temperatures at the three flow rates with and without degassing are shown in Fig. 5. Two regimes of behavior are easily identified, corresponding to single-phase liquid flow with a linear temperature increase with heat flux and to two-phase flow with a much smaller increase in wall temperature. The boiling inception temperature for the degassed liquid is well demarcated (104°C), and beyond this point, the temperature remains relatively constant. In the undegassed case, this demarcation is less sharp. Deviation from single-phase flow behavior, in this case, can be identified as the point at which the measured temperatures start to deviate from those for single-phase flow of the degassed liquid. This temperature for the undegassed liquid is much lower than in the degassed case. The temperature measurements for the two cases are seen to deviate significantly beyond a wall temperature of approximately 85°C when bubbles were observed to appear in all the microchannels. Beyond this temperature, there is a continued increase in wall temperature with increasing heat flux as seen in Fig. 5 for the undegassed liquid; also, the wall temperatures are higher at lower flow rates. This observation supports the analysis in the previous section that the initially observed bubbles in the undegassed liquid contain a significant portion of air. The formation of air-vapor bubbles alters the flow field and thus leads to "pseudo-boiling" as heat flux is further increased. A similar phenomenon was observed by Muller-Steinhagen et al. [6]. In this pseudo-boiling process, convective effects continue to play a significant role in the two-phase flow regime for the undegassed liquid.

Heat transfer coefficients for both the undegassed and degassed liquid at the three flow rates are presented in Fig. 6. As expected, since the flow is laminar at all the three flow rates (Re = 47, 63, 79, respectively, where $\text{Re} = \rho_l V D_h / \mu_l$), heat transfer coefficients for single-phase flow remain relatively constant and approximately the same. For the undegassed liquid, the heat transfer

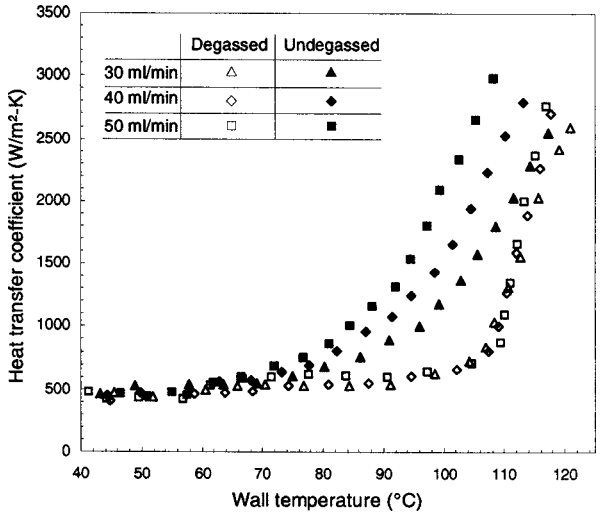

Fig. 6 Heat transfer coefficient for undegassed and degassed cases at three flow rates

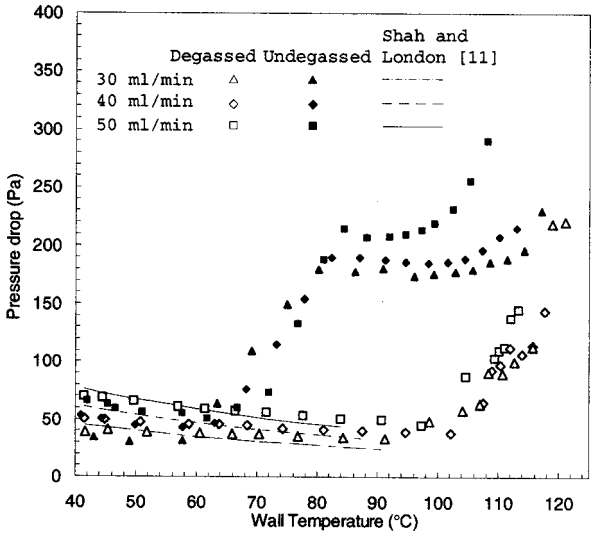

Fig. 7 Pressure drop at different wall temperatures for both degassed and undegassed liquid flow

coefficients start to increase at a much lower wall temperature, whereas for the degassed case, single-phase heat transfer sustains a wide range of temperature. The average Nusselt number for single-phase heat transfer (i.e., for wall temperatures below 75°C in Fig. 6) is calculated to be 6.77.

In order to facilitate a comparison of the present results against the literature, dimensionless thermal and hydrodynamic entrance lengths are calculated using

$$x^* = \frac{L}{\mathrm{Re}\,\mathrm{Pr}\,D_h} \tag{16}$$

$$x^+ = \frac{L}{\mathrm{Re}\,D_h} \tag{17}$$

and are shown in Table 2.

It is seen from Table 2 that hydrodynamically developed and thermally developing conditions exist in the present experiments, using the criteria that x^* and x^+ should be >0.05 for fully developed conditions. Also, since only three sides of the microchannels were heated in the present work, the approach used in Lee et al. [11] is adopted here to predict the Nusselt number in single-phase flow based on results in the literature that apply to all four sides of the microchannels being heated

$$\mathrm{Nu}_{x,3} = \mathrm{Nu}_{x,4}\frac{\mathrm{Nu}_{fd,3}}{\mathrm{Nu}_{fd,4}} \tag{18}$$

in which $\mathrm{Nu}_{x,4}$, $\mathrm{Nu}_{fd,3}$, and $\mathrm{Nu}_{fd,4}$ were given to be 6.35, 6.07, and 5.74, respectively, by Shah and London [12] for the geometry and boundary conditions considered. Thus, $\mathrm{Nu}_{x,3}$ is calculated to be 6.71 and seen to be in good agreement with the value of 6.77 obtained from measurements in this work.

A prominent effect of degassing is seen in that the heat transfer coefficient increases gradually in the undegassed case once boiling starts, whereas in the degassed liquid, the rise in heat transfer coefficient is very steep. This is again attributed to the air content in the bubbles formed in the undegassed liquid.

Table 2 Thermal and hydrodynamic entrance lengths

Re	x^*	x^+
47	0.039	0.38
63	0.029	0.48
79	0.023	0.64

Pressure Drop and Instability. The measured pressure drop between the inlet and outlet plenums represents contributions from the pressure drop due to flow in the microchannels as well as the inlet and exit losses. In the pressure-drop results presented in Fig. 7, the inlet and exit loss components are subtracted from the measured values according to the method of Liu and Garimella [13].

The pressure drop measurements in Fig. 7 again indicate the two distinct regimes of single-phase and two-phase flow. For single-phase hydrodynamically developed laminar flow in rectangular channels, the friction factor can be computed from Shah and London [12]

$$f_{\mathrm{laminar}}\,\mathrm{Re} = 24(1 - 1.3553\beta + 1.9467\beta^2 - 1.7012\beta^3 + 0.9564\beta^4 - 0.2537\beta^5) \tag{19}$$

in which β is the aspect ratio (W/H) of the rectangular channel, and f_{laminar} is the Fanning friction factor. For the aspect ratio of the microchannels studied, β is 0.2 and the product of $(f_{\mathrm{laminar}}\,\mathrm{Re})$ is calculated to be 19. The pressure drop can be calculated from

$$\Delta P = 2f_{\mathrm{laminar}}\frac{l}{D_h}\rho_l V^2 \tag{20}$$

in which the temperature-dependent density and viscosity are obtained from 3M Fluorinerts [1] as follows:

$$\rho(T) = 1838 - 2.45T \tag{21}$$

$$\mu(T) = -0.0005\ln(T) + 0.0027 \tag{22}$$

The calculated results from this method for single-phase flow at the three flow rates are also included in Fig. 7. It is noted that the flow is assumed to be uniformly distributed among all the microchannels in the heat sink and the pressure drop across any one single channel represents the total pressure drop. The calculated results are seen to be in satisfactory agreement with the measurements.

Corresponding to the appearance of bubbles in one or two microchannels, and then in more channels as the heat flux increases, a gradual increase in pressure drop is observed for both undegassed and degassed cases. As the formation of bubbles and development of two-phase flow patterns in different individual channels may occur at slightly different times, the pressure drop increases over a range of wall temperatures, rather than exhibiting an abrupt increase as might be expected for a single channel. As the boiling process becomes established in all the microchannels

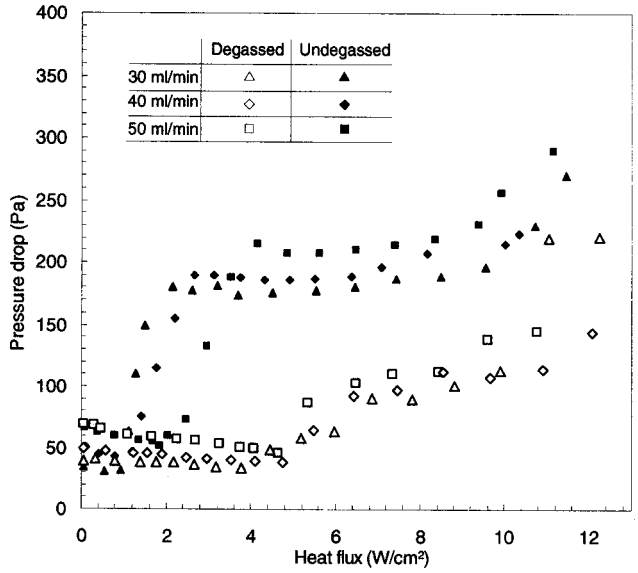

Fig. 8 Measured pressure drop at different heat fluxes for undegassed and degassed liquid flow

of the heat sink, the pressure-drop curve flattens out over a range of heat fluxes, as shown in Fig. 8. The pressure drop for the undegassed liquid is seen to be approximately two times larger than that for degassed liquid in this regime (from 6 to 8 W/cm^2).

Interesting flow instabilities were also visually observed with both the undegassed and degassed liquid. Some bubbles generated close to the channel inlet were periodically pushed back into the inlet manifold and then swept again into the channels. Periodic back-and-forth oscillation of bubbles before detaching from their nucleation sites was also observed. Such instabilities are reflected as an increased standard deviation in the measured pressure drop data (obtained with a time resolution of 1 s), defined as

$$\sigma_{\Delta p} = \sqrt{\frac{\sum_{i}^{N} (\Delta p_i - \overline{\Delta p})^2}{N}} \tag{23}$$

The standard derivation of pressure drop for the flow rate 50 ml/min is shown in Fig. 9. It is clear that the flow instability

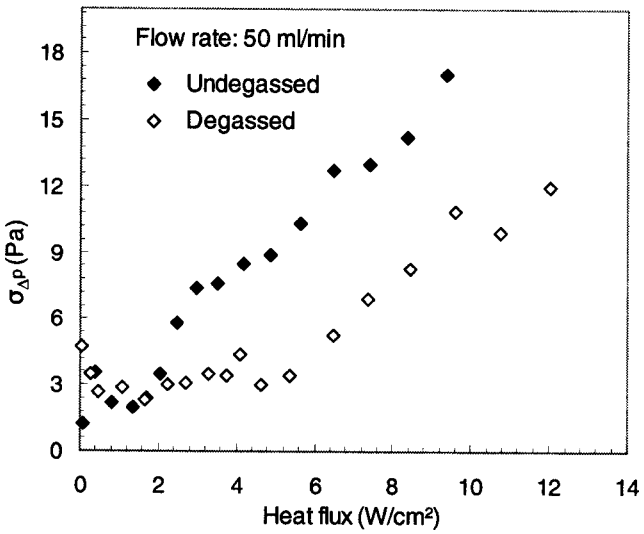

Fig. 9 Comparison of instability in the undegassed and degassed cases

increases as more vigorous boiling occurs (at higher heat fluxes) in both degassed and undegassed cases; the undegassed liquid produces the larger instabilities within the range of input heat flux considered in this work.

Summary and Conclusions

The effects of dissolved air on the flow boiling of the dielectric liquid FC-77 in a microchannel heat sink were experimentally investigated. A specially devised degassing scheme was developed that supplies degassed liquid to the flow loop while at the same time, providing control of the pressure in the test section. Degassing the liquid was found to have a strong impact on both the measured heat transfer and pressure drop. The following conclusions can be drawn from this study:

1. Boiling incipience temperatures were reduced from the saturation values at all three flow rates for undegassed liquid. The observed temperature for bubble incipience was lower than that predicted by a simple mechanical force model, suggesting that the initially observed bubbles are most likely air bubbles.
2. The wall temperature continued to increase after the boiling process was initiated in the undegassed liquid, in contrast to the wall temperature remaining relatively constant upon the initiation of boiling in the degassed liquid.
3. Earlier boiling inception in the microchannels with the undegassed liquid results in an earlier increase in heat transfer coefficients. However, at higher heat fluxes (>120 kW/m^2), the heat transfer coefficients for undegassed and degassed liquid reach similar values.
4. Larger pressure drops were measured for boiling with the undegassed liquid.
5. Flow instability, as quantified by the standard deviation in the measured pressure drop across the heat sink, increased with increasing heat flux and was higher for the undegassed liquid.

For application to electronics cooling, it is recommended that liquids be fully degassed to ensure greater predictability (and control) of wall temperature and to ensure lower pressure drops and flow instabilities.

Acknowledgment

Support for this work from the Indiana 21st Century Research and Technology Fund is gratefully acknowledged.

Nomenclature

A = microchannel heat sink base area (mm^2)
c_g = air concentration (mole/mole)
C_p = specific heat (J/kg K)
d = distance of thermocouples from bottom surface of microchannel (mm)
D_h = hydraulic diameter (mm)
H = microchannel depth (mm)
f = Fanning friction factor
h = heat transfer coefficient (W/m^2 K)
H_o = Henry's constant (mole/mole kPa)
k = thermal conductivity (W/m K)
L = microchannel length (mm)
M = molecular weight (g/mol)
N = number of data points
Nu = Nusselt number
P = pressure (Pa)
P_{atm} = atmospheric pressure (Pa)
Pr = Prandtl number
P_{vo} = vapor pressure at 25 °C (Pa)
$\dot{q}$ = heat transfer rate (W)
Q = flow rate (ml/min)

r = bubble embryo radius (μm)
Re = Reynolds number
T = temperature (°C)
V = velocity (mm/s)
$\bar{V}_{\text{mole}}$ = volume (1 mole) (mm^3)
W = microchannel width (mm)
x^* = dimensionless thermal entrance length
x^+ = dimensionless hydrodynamic entrance length

Greek Letters

β = aspect ratio
Δ = difference
ε = measurement uncertainty
μ = dynamic viscosity (kg/m s)
ρ = density (kg/mm^3)
σ = surface tension (N/m), standard deviation (Pa)

Subscript

3 = three sides heated
4 = four sides heated
cu = copper
fd = hydrodynamically developed flow
g = air
in = microchannel inlet
l = liquid
laminar = laminar flow
loss = heat loss
out = microchannel outlet
p = pressure
input = input
sat = saturation
sp = single phase
tp = two phase
v = vapor
w = microchannel wall
x = thermally developing flow

References

[1] 3M, 1995, *3M Fluorinert Liquids Product Manual*, 3M, St. Paul, MN.
[2] Torikai, K, Shimamunu, H., and Fujishiro, T., 1970, "The Effect of the Dissolved Gas Content Upon Incipient Boiling Superheats," *Proceedings of the 4th International Heat Transfer Conference*, Paris and Versailles, B2.11, Elsevier Publications, New York.
[3] Murphy, R. C., and Bergles, A. E., 1972, "Subcooled Flow Boiling of Fluorocarbons—Hysteresis and Dissolved Gas Effects on Heat Transfer," *Proceedings of Heat Transfer and Fluid Mechanics Inst.*, Stanford University Press, Stanford, pp. 400–416.
[4] You, S. M., Simon, T. W., Bar-Cohen, A., and Hong, Y. S., 1995, "Effect of Dissolved Content on Pool Boiling of a Highly Wetting Fluid," ASME J. Heat Transfer, **117**, pp. 687–692.
[5] Hong, Y. S., Ammerman, C. N., and You, S. M., 1997, "Boiling Characteristics of Cylindrical Heaters in Saturated, Gas-Saturated, and Pure-Subcooled FC-72," ASME J. Heat Transfer, **119**, pp. 313–318.
[6] Muller-Steinhagen, H., Epstein, N., and Watkinson, A. P., 1988, "Effect of Dissolved Gases on Subcooled Flow Boiling Heat Transfer," Chem. Eng. Process., **23**, pp. 115–124.
[7] Steinke, M. E., and Kandlikar, S. G., 2004, "Control and Effect of Dissolved Air in Water During Flow Boiling in Microchannels," Int. J. Heat Mass Transfer, **47**, pp. 1925–1935.
[8] Kline, S. J., and McClintock, F. A., 1953, "Describing Uncertainties in Single-Sample Experiments," Mech. Eng. (Am. Soc. Mech. Eng.), **75**, pp. 3–8.
[9] Chen, J. C., 1966, "A Correlation for Boiling Heat Transfer to Saturated Fluids in Convective Flow," Ind. Eng. Chem. Prod. Res. Dev., **5**, pp. 322–329.
[10] Hsu, Y. Y., 1962, "On the Size Range of Active Nucleating Cavities on a Heating Surface," ASME J. Heat Transfer, **84**, pp. 207–213.
[11] Lee, P. S., Garimella, S. V., and Liu, D., 2005, "Investigation of Heat Transfer in Rectangular Microchannels," Int. J. Heat Mass Transfer, **48**, pp. 1688–1704.
[12] Shah, R. K., and London, A. L., 1978, *Laminar Flow Forced Convection in Ducts*, Supplement 1 to *Advances in Heat Transfer*, Academic Press, New York.
[13] Liu, D., and Garimella, S. V., 2004, "Investigation of Liquid Flow in Microchannels," J. Thermophys. Heat Transfer, **18**, pp. 65–72.